



Lipid Biomarkers and Their Stable Carbon Isotopes in Ancient Seep Carbonates from SW Taiwan, China

GUAN Hongxiang^{1,2,*}, XU Lanfang^{1,3}, WANG Qinxian⁴, CHEN Duofu^{2,4},
WU Nengyou² and MAO Shengyi¹

¹ Key Laboratory of Gas Hydrate, Guangzhou Institute of Energy Conversion, Chinese Academy of Sciences, Guangzhou 510640, Guangdong, China

² Laboratory for Marine Mineral Resources, Qingdao National Laboratory for Marine Science and Technology, Qingdao 266061, Shandong, China

³ University of Chinese Academy of Sciences, Beijing 100049, China

⁴ Shanghai Engineering Research Center of Hadal Science and Technology, College of Marine Sciences, Shanghai Ocean University, Shanghai 201306, China

Abstract: Four massive brecciated, chimney-like, and slender pipe network carbonate samples (JA-4, JA-5, JX-8 and BG-12) were collected from southwestern Taiwan, which were suggested to have formed as a result of anaerobic oxidation of methane (AOM). Considering that the environmental conditions of the carbonates precipitation and the sources of carbon and organic matter need to be further declared, molecular fossils and compound-specific carbon isotopic investigations of the carbonates were conducted in this study. According to lipid biomarkers of 2,6,10,15,19-pentamethyleicosane (PMI) and squalane diagnostic to methanotrophic archaea, as well as the extremely low $\delta^{13}\text{C}$ values (as low as -113.4‰) detected in samples JA-4, JA-5 and JX-8, these carbonates were revealed to be a result of AOM. Based on the varied $\delta^{13}\text{C}$ values of characteristic archaea biomarkers in specific samples, biogenic methane was proposed to be responsible for the formation of samples JA-4 and JA-5, whereas a mixed carbon source of ^{13}C -depleted methane and ^{13}C -enriched residual CO_2 from methanogenesis was suggested for the carbonate of JX-8 due to the co-occurrence of a highly positive $\delta^{13}\text{C}_{\text{carb}}$ value ($+8\text{‰}$) and a moderate ^{13}C depletion of PMI. The low content of AOM-related biomarkers and the absence of indicators for ANME-2 suggested that these carbonates were formed in weak seep settings. By comparison, no typical lipid biomarkers for methanotrophic archaea were detected in carbonate BG-12. The short-chain and long-chain *n*-alkanes accounted for 30% and 45% of all hydrocarbons, respectively, with a CPI value of 1.2, suggesting that the *n*-alkanes were derived from both marine organisms and terrestrial inputs. A low thermal maturity could be revealed by the incomplete equilibrium value of the $\text{C}_{31}\alpha\beta$ 22S/(22S+22R) ratio (0.5), and the carbonate BG-12 was probably deposited in a suboxic condition indicated by a value of Pr/Ph ratio (2.5).

Key words: methane seeps, lipid biomarkers, anaerobic oxidation of methane, weak seep settings

Citation: Guan et al., 2019. Lipid Biomarkers and Their Stable Carbon Isotopes in Ancient Seep Carbonates from SW Taiwan. *Acta Geologica Sinica* (English Edition), 93(1): 167–174. DOI: 10.1111/1755-6724.13772

1 Introduction

Hydrocarbon seepage is common in marine environments worldwide (Campbell, 2006; Judd and Hovland, 2007; Boetius and Wenzhöfer, 2013). Anaerobic oxidation of methane (AOM) is a key process that occurs at seeps and favors the precipitation of authigenic carbonates (Barnes and Goldberg, 1976; Reeburgh, 1976, 1996; Boetius et al., 2000; Hinrichs et al., 2000; Feng et al., 2010, 2014; Suess, 2014). AOM at cold seeps is performed by a consortium of anaerobic methane-oxidizing archaea and sulfate-reducing bacteria (Boetius et al., 2000). Usually, archaeal membrane lipids strongly depleted in ^{13}C are prevalent in modern seep carbonates from vigorous cold seep sites (Niemann and Elvert, 2008), whereas lipid biomarkers for terrestrial and marine environments indicate the major organismal inputs for

seep carbonates from weak seep settings or ancient limestones (Peckmann et al., 2009; Blumenberg et al., 2015; Guan et al., 2016a). Accordingly, the inherent nature of seep is that fluid flow intensity is highly variable both spatially and temporally. It was previously suggested that carbonate mineralogy and lipid biomarkers can be used to reconstruct seepage intensity (Peckmann et al., 2009; Birgel et al., 2011; Nöthen and Kasten, 2011; Feng et al., 2016; Guan et al., 2016b). For example, abundant crocetane and a high ratio of *sn*2-hydroxyarchaeol/archaeol have been reported in most ANME-2-dominated seep settings and carbonates, representing seep ecosystems with high methane intensities (Blumenberg et al., 2004; Birgel et al., 2011; Guan et al., 2013; Himmler et al., 2015). Moreover, the $\delta^{13}\text{C}$ value of methane can also be achieved by compound-specific carbon isotopes based on different fractionations between methane and lipids in specific microbial communities (cf. Niemann and Elvert,

* Corresponding author. E-mail: guanhx@ms.giec.ac.cn

2008). Therefore, lipid contents, distribution patterns and compound-specific carbon isotopes are commonly used to assess environmental conditions and the sources of carbon and organic matter.

In recent years, modern methane-seeps, authigenic carbonates (Huang et al., 2006) and mud volcanoes (Chiu et al., 2006) were reported to be on the Kaoping Slope of southwestern Taiwan. Furthermore, several fossilized, cold-seep carbonates are also preserved onshore in southwestern Taiwan (Wang et al., 2006; Chien et al., 2012). Among those reports, the occurrence of authigenic carbonates and their mineralogy, petrography, and stable carbon and oxygen isotopic compositions have been reported (Chiu et al., 2006; Huang et al., 2006; Wang et al., 2006; Chien et al., 2012, 2013; Wang et al., 2018). Nonetheless, the environmental conditions of the carbonates precipitation and the sources of carbon and organic matter remained unclear. Here, we investigated the lipid biomarker inventories and their $\delta^{13}\text{C}$ values in carbonates from the Chiahsien area of southwestern Taiwan to identify the environments in which the carbonates precipitated and the sources of carbon and organic matter.

2 Geological Setting and Sample Description

The orogeny of Taiwan Island resulted from the collision between the Eurasian plate and the Philippine Sea plate (Suppe, 1984). The Western Foothills of Taiwan, consisting of late Oligocene to Pleistocene shallow marine strata, deposited on the stable passive continental margin (Lin et al., 2003). It is equivalent to the syn-collision accretionary prism, the Kaoping Slope, of southwestern Taiwan (Huang et al., 2001). There are many cold seep sites (Huang et al., 2006), mud volcanoes (Chiu et al., 2006) and cold seep remnants from the Miocene (Chien et al., 2012) to the Pleistocene (Wang et al., 2006) on the Kaoping Slope. Several ancient seep carbonates have also been found in the Western Foothills (Wang et al., 2006; Chien et al., 2013; Wang et al., 2018). The Chiahsien area is located at the foreland basin within the Western Foothills Zone. The strata in the Chiahsien area varies from the Late Miocene Tangenshan Fm. to the Ailiaochiao Fm. (Chung, 1962). Thrust faults, synclines and anticlines are extensively developed in the Chiahsien area.

Authigenic carbonate samples were collected from the Chiahsien area (Fig. 1). The ancient cold seep carbonate is within the Yenshuikeng Shale, located between the low-angled Pinghsi Thrust Fault and the high-angled Chishan Thrust Fault (Sung et al., 2000; Chien et al., 2013). Authigenic carbonate from the Pliocene marine mudstone succession is exposed near the Chiahsien area (Fig. 2). These carbonates were collected from three exposures (Exposure A, B and C; see Fig. 1). They displayed different types of morphologies, including massive brecciated blocks, chimney-like structures, slender pipe networks (Chien et al., 2013), which are usually perpendicular to the bedding. They are mainly composed of dolomite with minor amounts of calcite. Samples JA-4 and JA-5 were collected from Exposure A (Fig. 1) and characterized by chimney-like structures (diameters

usually >15 cm). JX-8 was sampled from Exposure B and represented by massive structures (typically 2.0 to 4.0 m in length, 1.0 to 2.0 m in width, 3.0 to 5.0 m in height). BG-12 was collected from Exposure C (Bai-yun-xian-gu), approximately 3 km to the east of the Chiahsien Township and characterized by blocks and irregular-shaped concretions. In addition, chemosymbiotic lucinids plecyopods *Anodontia goliath* were found in exposures A and C (Taylor and Glover, 2009; Chien et al., 2013). The $\delta^{13}\text{C}_{\text{carb}}$ values for JA-4, JA-5 and BG-12 were extremely negative, varying from -39‰ to -27‰ , while JX-8 was enriched in ^{13}C with a $\delta^{13}\text{C}_{\text{carb}}$ value of $+8\text{‰}$ (Wang et al., 2018). The $\delta^{18}\text{O}$ values ranged from -1‰ to $+2\text{‰}$ in samples JA-4, JX-8 and BG-12, whereas sample JA-5 had the lowest $\delta^{18}\text{O}$ value of -9‰ (Wang et al., 2018).

3 Methods

Four authigenic carbonate samples, BG-12, JA-4, JA-5 and JX-8, were chosen for biomarker analysis. The method for preparation and extraction of lipids has been detailed by Guan et al. (2013). An aliquot of total lipid extracts (TLE) was saponified (with 6% KOH (w/v) in methanol), the neutral lipid fraction was then separated from the carboxylic acids by extracting the saponified TLE. The neutral lipid fraction was separated by column chromatography into three classes: (1) aliphatic hydrocarbons (*n*-hexane), (2) aromatic hydrocarbons (*n*-hexane/dichloromethane, 6:4; v:v) and (3) alcohols (methanol). The nitrogen-dried alcohols were converted to trimethylsilyl (TMS) derivatives by bis(trimethylsilyl) trifluoroacetamide (BSTFA) at 70°C for 1 hour prior to Gas Chromatography-Mass Spectrometry (GC-MS) analysis. To obtain the carboxylic acids, the saponified residuals were treated with 10% HCl to reach a pH of 2 and extracted by *n*-hexane until the solvents became colorless. Fatty acids methyl esters (FAMES) were transformed from free fatty acids by subjecting the dried fatty acid fraction to 14% BF_3 -methanol in a screwcap vial (2 hours, 60°C). All fractions were analyzed at the Guangzhou Institute of Energy Conversion, Chinese Academy of Sciences (GIEC, CAS), using a Thermo Electron Trace GC-MS equipped with a 60 m DB-5 MS, fused silica capillary column (0.32 mm i.d., 0.25 μm film thickness). Helium was supplied as the carrier gas at a flow rate of 1.2 ml/min. The following GC temperature programs were used: injection at 60°C with 2 min isothermal, heating from 60°C to 150°C at 10°C/min, heating from 150°C to 320°C at 4°C/min, and isothermal holding for 30 min for hydrocarbons and 40 min for FAMES and TMS-derivatives. Likewise, compound-specific carbon isotope analysis was performed on a GV Isoprime system interfaced to a Hewlett-Packard 6890 gas chromatograph at the Guangzhou Institute of Geochemistry, Chinese Academy of Sciences (GIG, CAS). The GC conditions were the same to those used in the GC-MS analysis. The stable carbon isotopic composition is expressed in the standard δ -notation in per mil (‰) relative to the Vienna-PeeDee Belemnite (V-PDB) standard. The FAMES and TMS-derivatives were corrected for the addition of carbon during preparation.

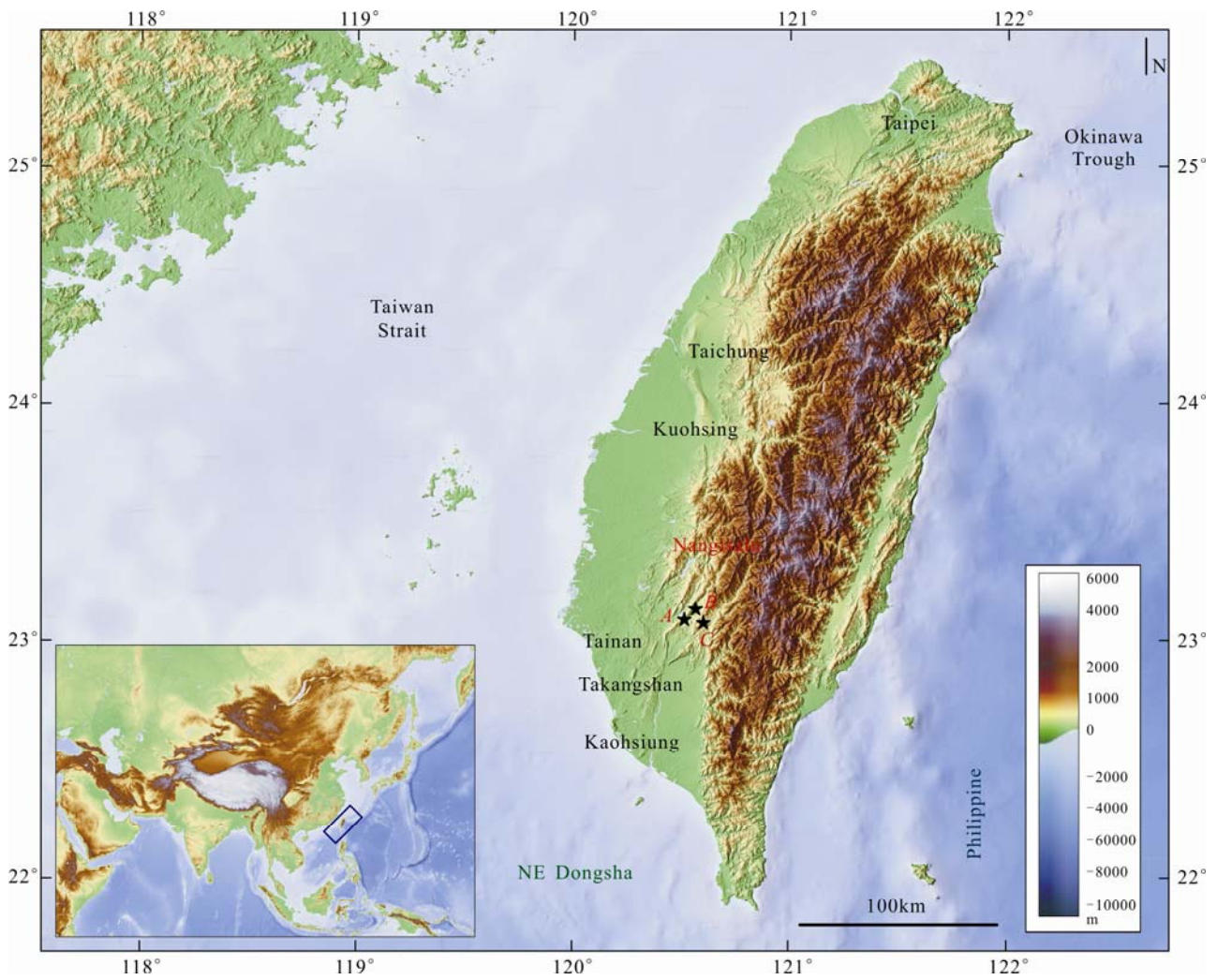


Fig. 1. Map of Taiwan showing the locations of the ancient seep carbonates in this study.

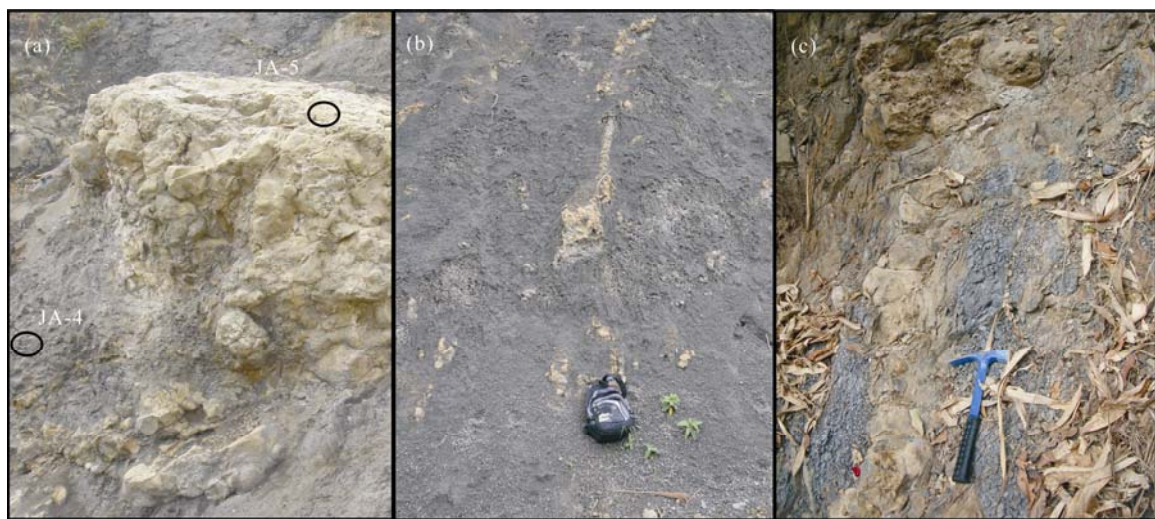


Fig. 2. Field photographs of carbonate samples collected from southwestern Taiwan. (a) JA-4 and JA-5, carbonates in gray mounds, surrounded by mudstones within small enticle carbonates. Carbonate chimneys were found in the upper regions of the mudstones. (b) JX-8, authigenic carbonate concretions. (c) BG-12, blocks and irregular-shaped concretions.

Each sample was analyzed at least in duplicate. The standard deviation of compound-specific carbon isotope measurements was <0.9‰.

4 Results and Discussion

4.1 Sources of organic matters

4.1.1 Based on hydrocarbons

Hydrocarbons were the most abundant class of organic compounds, whereas only a few polar lipid biomarkers were preserved in the carboxylic acid and alcohol fractions. The predominant hydrocarbons were *n*-alkanes with chain lengths from C₁₄ to C₃₆, peaking at *n*-C₁₇ and *n*-C₂₇, with bimodal distributions in sample BG-12 (Fig. 3). By contrast, the *n*-alkanes in the total ion chromatograms (TIC) of carbonate samples JA-4, JA-5 and JX-8 were characterized by unimodal distributions with *n*-C₁₆/*n*-C₁₇ as the most abundant components. In addition to the *n*-alkanes, isoprenoids of pristane and phytane were the most abundant isoprenoids with δ¹³C values ranging from -30.6‰ to -48.0‰ (Fig. 2; Table 1).

Lipid biomarkers are compounds that characterize certain biotic sources and retain their source information after burial in sediments, even after alteration (Meyers, 2003). In sample BG-12, short-chain and long-chain *n*-alkanes accounted for 30% and 45% of all hydrocarbons (*n*-C₂₂₊/*n*-C₂₁=1.5), respectively and have a carbon preference index (CPI) value of 1.2 (Table 1). The

presence of short odd alkanes, particularly with a maximum at *n*-C₁₇, is indicative of marine organisms such as algae, photosynthetic bacteria and marine animals (Blumer et al., 1971; Giger et al., 1980; Cranwell et al., 1987; Meyers, 2003; Mille et al., 2007). The long-chain *n*-alkanes, with C₂₃-C₃₆ maximized at *n*-C₂₇ and δ¹³C values of around -30‰, suggested that these compounds were mainly derived from leaf waxes of higher plants (Eglinton et al., 1962; Eglinton and Hamilton, 1963; Simoneit, 1977; Naraoka and Ishiwatari, 2000). The ratio of Pr/Ph was used as an indicator of the redox environment (Peters et al., 2005). The high ratio of Pr/Ph (2.5) found for BG-12 indicated that this carbonate formed under typical suboxic conditions. Based on the lack of isoprenoids diagnostic for ANMEs, the biomarker patterns and stable carbon isotopic compositions indicated that the carbonate BG-12 probably precipitated in a suboxic marine environment with a considerable contribution from terrestrial organisms.

In samples JA-4, JA-5 and JX-8, the short-chain *n*-alkanes represented approximately 50% of all hydrocarbons, and long-chain *n*-alkanes accounted for on average 25% of total hydrocarbons. The predominance of short-chain hydrocarbons and the low ratios of *n*-C₂₂₊/*n*-C₂₁ (0.5 to 0.9) suggested that the hydrocarbons mainly originated from marine organisms (Blumer et al., 1971; Giger et al., 1980; Cranwell et al., 1987; Meyers, 2003; Mille et al., 2007). The Pr/Ph ratios were relatively constant among samples and fell within a range of 0.6 to

Table 1 Stable carbon isotopic compositions of hydrocarbons analyzed and their relative percentages

Sample ID	JA-4		JA-5		JX-8		BG-12	
	Relative Percentages	δ ¹³ C (‰) V-PDB	Relative Percentages	δ ¹³ C (‰) V-PDB	Relative Percentages	δ ¹³ C (‰) V-PDB	relative percentages	δ ¹³ C (‰) V-PDB
<i>n</i> -C ₁₄	1.1	-31.4	n.d.	n.d.	n.d.	n.d.	1.3	-28.4
<i>n</i> -C ₁₅	3.7	-31.5	2.5	n.d.	1.0	n.d.	3.4	-30.6
<i>n</i> -C ₁₆	11.7	-32.1	10.7	-33.6	8.6	-28.8	5.8	-30.3
<i>n</i> -C ₁₇	10.0	-32.1	11.3	-34.3	9.4	-31.1	5.8	-29.9
Pristane	11.1	-32.4	7.8	-34.2	8.2	-32.9	17.2	-30.6
<i>n</i> -C ₁₈	10.5	-31.2	11.1	-33.6	9.2	-29.7	4.5	-29.9
Ph/Cr	12.4	-42.6	13.6	-48.0	8.5	-44.0	7.0	-33.4
<i>n</i> -C ₁₉	4.4	-35.1	5.1	-37.6	5.4	-31.4	3.2	-32.7
<i>n</i> -C ₂₀	4.2	-31.3	5.9	-33.6	7.4	-29.3	2.9	-30.8
<i>n</i> -C ₂₁	2.9	-35.3	3.5	-38.5	5.3	-30.3	3.2	-30.6
<i>n</i> -C ₂₂	2.6	-33.3	3.2	-34.9	4.9	-29.3	3.1	-31.4
PMI	2.3	-109.8	3.8	-113.4	1.5	-87.7	0	n.d.
<i>n</i> -C ₂₃	4.1	-59.8	4.8	-65.2	5.8	-40.8	3.5	-32.4
<i>n</i> -C ₂₄	2.1	-33.0	2.3	-38.8	3.8	-30.6	3.5	-31.8
<i>n</i> -C ₂₅	2.5	-35.9	2.2	-42.1	3.7	-30.6	4.2	-31.6
<i>n</i> -C ₂₆	2.0	-30.3	1.8	-37.3	2.7	-29.6	4.3	-31.7
Squalane	1.3	-96.4	1.7	-94.2	1.9	-74.4	0.5	n.d.
<i>n</i> -C ₂₇	2.1	-32.4	1.8	-34.1	3.0	-33.9	5.2	-32.4
<i>n</i> -C ₂₈	1.9	-32.5	1.3	-31.7	2.2	-31.0	4.6	-32.4
<i>n</i> -C ₂₉	1.9	-33.2	1.6	-38.0	2.9	-31.7	4.6	-32.3
<i>n</i> -C ₃₀	1.0	-31.2	1.1	-29.5	1.8	-3.3	3.2	-31.7
<i>n</i> -C ₃₁	1.3	-27.3	1.4	-31.7	2.5	n.d.	3.7	-32.6
<i>n</i> -C ₃₂	0.6	-34.0	0.7	n.d.	1.0	n.d.	2.0	-33.7
<i>n</i> -C ₃₃	0.9	-41.5	0.8	n.d.	1.3	n.d.	1.9	-32.6
<i>n</i> -C ₃₄	0.5	-46.7	n.d.	n.d.	n.d.	n.d.	0.8	-33.7
<i>n</i> -C ₃₅	0.5	-53.0	n.d.	n.d.	n.d.	n.d.	0.6	n.d.
<i>n</i> -C ₃₆	0.2	n.d.	n.d.	n.d.	n.d.	n.d.	0.2	n.d.
δ ¹³ C _{carb.}		-39‰		-34‰		+8‰		-27‰
δ ¹⁸ O _{carb.}		+2‰		-9‰		-1‰		0.9‰
Pristane/ <i>n</i> -C ₁₇	1.1		0.7		0.9		3.0	
Pr/Ph	0.9		0.6		1.0		2.5	
<i>n</i> -C ₂₂₊ / <i>n</i> -C ₂₁	0.5		0.8		0.9		1.5	
*CPI	1.3		1.3		1.5		1.2	
^a C ₃₁ αβ 22S/(22S+22R)	0.5		0.5		0.5		0.5	

$$*CPI = \frac{1}{2} \left[\frac{C_{25}+C_{27}+C_{29}+C_{31}+C_{33}}{C_{24}+C_{26}+C_{28}+C_{30}+C_{32}} + \frac{C_{25}+C_{27}+C_{29}+C_{31}+C_{33}}{C_{26}+C_{29}+C_{30}+C_{32}+C_{34}} \right]$$

Ph/C, Phtane/Crocetane; ^aC₃₁αβ 22S/(22S+22R), C₃₁homohopane 22S/(C₃₁homohopane 22S+C₃₁homohopane 22R). n. d.: not detected

1.0, which was normally interpreted as anoxic conditions (Harris et al., 2004). Further evidence in support of this conclusion came from the characteristic lipid biomarkers of AOM and their pronounced ^{13}C depletions.

4.1.2 Based on hopanoids

Hopanoids, mainly biosynthesized by some prokaryotes (Rohmer et al., 1984) and used as biomarkers for bacteria (Peters and Moldowan, 1991; Peters et al., 2005; Zhang et al., 2017; Li et al., 2017), are present ubiquitously in soils and sediments (Rohmer et al., 1984; Peters and Moldowan, 1991; Peters et al., 2005; Guan et al., 2014). A series of C_{27} – C_{34} hopanes were detected in all samples with $17\alpha(\text{H}),21\beta(\text{H})$ -hopanes being the most abundant biomarkers (Fig. 4; Table 2). Among these samples, the concentrations of extended C_{31} – C_{34} hopanes decreased towards the C_{34} pseudohomologue (Fig. 4). In addition, relatively low contents of moretanes and “biological” $17\beta(\text{H}),21\beta(\text{H})$ -hopanes were also present.

The numerous organic compounds present in carbonates suggested that no heavy alteration occurred compared to modern seep carbonates (Birgel et al., 2006). Based on the biomarker patterns and compositions, the double bonds and unstable structures were destroyed by hydrogenation of double bonds substitution of hydrogen for hydroxyl or aromatization of rings (Meyers, 2003). As shown in Table 1, all $\text{C}_{31}\alpha\beta$ $22\text{S}/(22\text{S}+22\text{R})$ ratios were 0.5, suggesting a relatively lower thermal maturity (Peters et al., 2005; Birgel et al., 2006).

4.2 Biomarkers diagnostic for AOM and formation of the authigenic carbonates

Samples JA-4, JA-5 and JX-8 contained typical lipid biomarkers diagnostic for methanotrophic archaea. The isoprenoid hydrocarbons of 2,6,10,15,19-pentamethylicosane (PMI) and squalane with strong ^{13}C -depletions in samples JA-4, JA-5 and JX-8 suggested that the primary carbon source was methane, which was primarily oxidized in an anaerobic process (Sackett, 1978; Whiticar et al., 1986; Elvert et al., 1999, 2000; Hinrichs et al., 2000; Boetius et al., 2000; Blumenberg et al., 2004; Guan et al., 2013, 2016b). Among these samples, the isoprenoid hydrocarbons PMI and squalane diagnostic for methanotrophic archaea were present in low percentages less than 6% of all hydrocarbons. Usually, crocetane is used as an indicator for ANME-2/DSS consortia since it is abundant in ANME-2/DSS-dominated habitats and only present in trace amounts or absent in ANME-1/DSS-dominated ecosystems (Niemann and Elvert, 2008). In samples JA-4, JA-5 and JX-8, crocetane co-eluted with phytane with minor contributions to the combined peaks,

which can be indicated by the slightly lower $\delta^{13}\text{C}$ values relative to pristane since $\delta^{13}\text{C}$ values of pure phytane usually falls in the same range as pristane in the same sample. The lipid biomarkers from terrestrial and marine environments were indicated as the major organismal

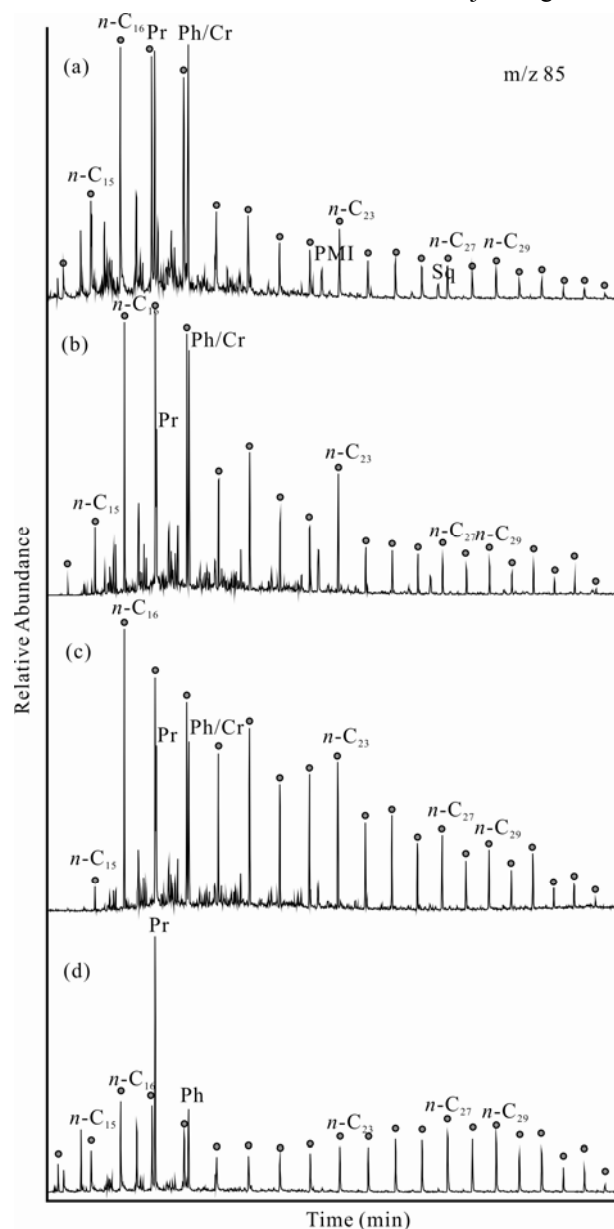


Fig. 3. Partial gas chromatograms (FID) of hydrocarbon fractions of samples (a) JA-4, (b) JA-5, (c) JX-8, and (d) BG-12. Cr: crocetane; PMI: 2,6,10,15,19-pentamethylicosane; Pr: pristane; Ph: phytane; Sq: squalane. Gray dots: *n*-alkanes.

Table 2 Detected hopanoid compounds showed in chromatogram of m/z 191 in authigenic carbonates

Number	Biomarkers	Number	Biomarkers
1	18 α (H),22,29,30-trisnorhopane(Ts)	10	17 β (H)-21 β (H)-hopane
2	17 α (H),22,29,30-trisnorhopane(Tm)	11	22R-17 β (H),21 α (H)-30-homomoretane
3	17 α (H),21 β (H)-30-norhopane	12	22S-17 α (H),21 β (H)-bihomohopane
4	17 β (H),21 α (H)-30-normoretane	13	22R-17 α (H),21 β (H)-bihomohopane
5	18 α (H)-oleanane	14	22S-17 α (H),21 β (H)-trihomohopane
6	17 α (H),21 β (H)-hopane	15	22R-17 α (H),21 β (H)-trihomohopane
7	17 β (H),21 α (H)-moretane	16	22S-17 α (H),21 β (H)-tetrahomohopane
8	22S-17 α (H),21 β (H)-30-homohopane	17	22R-17 α (H),21 β (H)-tetrahomohopane
9	22R-17 α (H),21 β (H)-30-homohopane		

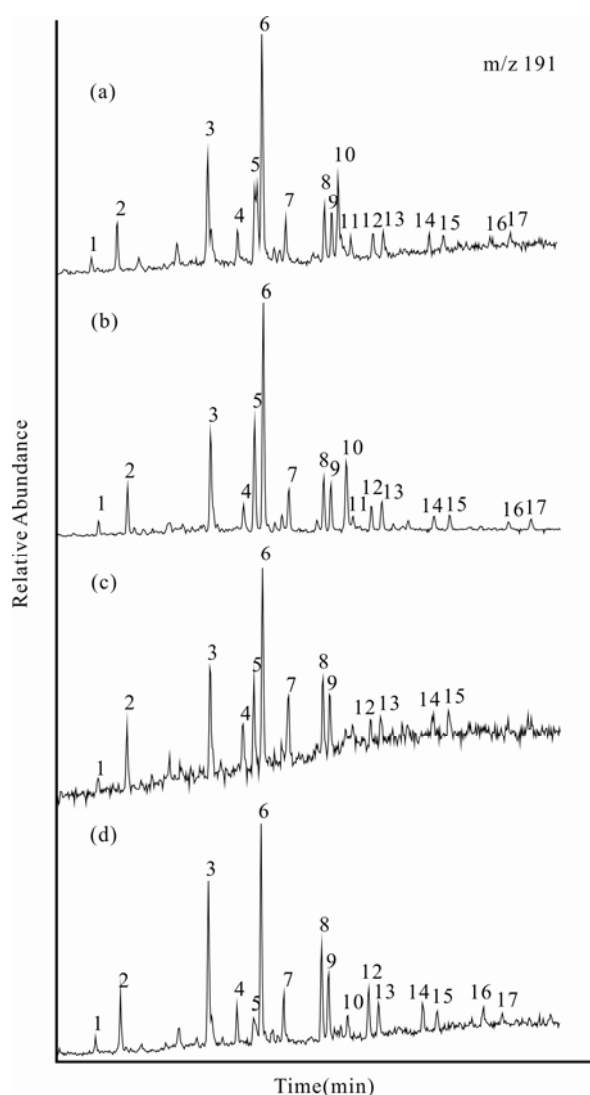


Fig. 4. Partial gas chromatograms of hopanoid compounds (m/z 191) from samples (a) JA-4, (b) JA-5, (c) JX-8, and (d) BG-12.

Arabic numbers indicate the corresponding compounds in Table 2.

inputs for seep carbonates from weak seep settings or ancient limestones (Peckmann et al., 2009; Guan et al., 2016a). In the present study, lipid biomarkers from terrestrial and marine environments dominated over hydrocarbons (by more than 70%). This together with the low contents of AOM-related biomarkers, as well as the lack of indicators for ANME-2, suggested that the carbonates precipitated in weak seep settings.

Apart from the isoprenoid hydrocarbons PMI and squalane, *n*-tricosane was present in carbonates JA-4, JA-5 and JX-8 with moderate ^{13}C -depletions ranging from -65.2% to -40.8% . *n*-Tricosane with moderate ^{13}C -depletion has been reported at modern cold seep deposits, associated microbial mats and ancient methane seep limestones (Thiel et al., 2001; Peckmann et al., 2009; Chevalier et al., 2013), which has been suggested to be AOM-associated and even maybe produced by archaea (Thiel et al., 2001). However, Chevalier et al. (2013) reported a co-occurrence of ^{13}C -depleted 7,14-tricosadiene

and JS1 bacteria at the AOM interval in a sediment core from the sea of Marmara (Turkey). Although no bacterial Candidate Division JS1 has been cultivated so far, the strongly ^{13}C -depleted signature and structure of the tricosane and related unsaturated tricosenes make bacterial Candidate Division JS1 indeed a potential source candidate for tricosane (cf., Chevalier et al., 2013).

In seep carbonates JA-4 and JA-5, the irregular isoprenoid hydrocarbons PMI and squalane revealed strong ^{13}C -depletion with $\delta^{13}\text{C}$ values ranging from -113.4% to -94.2% , whereas they showed relatively higher $\delta^{13}\text{C}$ values between -87.7% and -74.4% in carbonate JX-8. Since methanotrophic archaea could have a strong fractionation of stable carbon isotopes between membrane lipids and the source methane, $\Delta\delta^{13}\text{C}_{\text{lipid-methane}}$ values of archaea biomarkers compared to the source methane often range between -30% to -50% on average for ANME-1 and ANME-2 (Niemann and Elvert, 2008), which has been testified on carbonates from modern seep sites (Birgel et al., 2011; Himmler et al., 2015). Based on the $\delta^{13}\text{C}$ values of PMI in samples JA-4 and JA-5, calculated $\delta^{13}\text{C}_{\text{methane}}$ values below -60% are obtained either by ANME-1- or ANME-2-domination, suggesting a microbial methane was involved in the precipitation of both carbonates (Whiticar, 1999). In terms of JX-8, the $\delta^{13}\text{C}_{\text{methane}}$ value ranged from -39% to -58% , indicating a thermogenic origin was likely. However, the heavy $\delta^{13}\text{C}_{\text{carb}}$ value of $+8\%$ for carbonate JX-8 could be served as an evidence for additional carbon sources. In sediments below the sulfate–methane transition zone (SMTZ), continued CO_2 -reduction in an almost closed system drives methanogenesis which results in a ^{13}C -enriched CO_2 pool (Lapham et al., 2008). Seep carbonates are usually characterized by low $\delta^{13}\text{C}$ values. However, $\delta^{13}\text{C}$ values higher than $+5\%$ have been reported for some ancient seep carbonates (Budai et al., 2002; Peckmann and Thiel, 2004; Chien et al., 2013; Wang et al., 2018). In the present study, the highly positive $\delta^{13}\text{C}$ value of $+8\%$ together with the moderate ^{13}C -depletion of PMI and squalane suggested that carbonate JX-8 formed from a mixed carbon source of ^{13}C -depleted methane and ^{13}C -enriched residual CO_2 from methanogenesis. A large $\delta^{13}\text{C}$ offset between GDGT-0 (based on acyclic biphytane) and other GDGTs (based on cyclic biphytanes) has been reported in authigenic carbonates from the Gulf of Mexico (GoM), which has been attributed to a contribution from methanogenic Euryarchaeota (Feng et al., 2014). Relative to the extreme ^{13}C -depletion of archaea biomarkers and the moderately negative $\delta^{13}\text{C}_{\text{carb}}$ values (-29.8% to -18.1%) in the carbonates from the GoM, the moderately ^{13}C -depleted archaea biomarkers and the positive $\delta^{13}\text{C}_{\text{carb}}$ value preserved in carbonate JX-8 stress the need for further investigation on geochemical mechanisms for the co-occurrence of methanogenesis and AOM.

5 Conclusions

The limestones of JA-4, JA-5 and JX-8 from SW Taiwan contained strongly ^{13}C -depleted archaea isoprenoid hydrocarbons that demonstrated the occurrence of microbial communities responsible for anaerobic

oxidization of methane. Based on the $\delta^{13}\text{C}$ values of PMI, calculated $\delta^{13}\text{C}_{\text{methane}}$ values below -60‰ are obtained for exposure A (JA-4 and JA-5), which suggested that a microbial methane was involved in AOM during the precipitation of the seep carbonates, whereas a mixture of ^{13}C -depleted methane and ^{13}C -enriched residual CO_2 from methanogenesis seem likely for exposure B (JX-8). In addition, the predominance of short-chain *n*-alkanes and relatively low ratios of $n\text{-C}_{22}/n\text{-C}_{21}$ (0.5 to 0.9) revealed that hydrocarbons mainly originated from marine organisms. The low contents of AOM-related biomarkers as well as the absence of the indicators for ANME-2 suggested that the seep carbonates formed in weak seep settings. The presence of *n*-alkanes with bimodal distribution patterns and particular maxima at $n\text{-C}_{17}$ and $n\text{-C}_{27}$ suggested that lipid biomarkers of carbonate BG-12 chiefly derived from marine organisms and leaf waxes from higher plants. The $\text{C}_{31}\alpha\beta/22\text{S}/(22\text{S}+22\text{R})$ ratio of 0.5 indicated that the organic matter was of lower thermal maturity and this sample probably formed at suboxic conditions as revealed by a Pr/Ph index of 2.5.

Acknowledgments

We thank Prof. C.Y. Huang (National Cheng Kung University, Taiwan) for the collection of these samples. We are grateful to Dr. L. Liu and the two reviewers for their comments, which considerably improved the quality of the manuscript. This study was supported by Qingdao National Laboratory for Marine Science and Technology (No. QNLM2016ORP0210) and the NSF of China (No. 41473080 and 41673029).

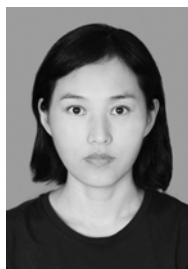
Manuscript received Jun. 21, 2018
accepted Aug. 27, 2018
associate EIC HAO Ziguo
edited by LIU Lian

References

- Barnes, R.O., and Goldberg, E.D., 1976. Methane production and consumption in anoxic marine sediments. *Geology*, 4(5): 297–300.
- Birgel, D., Feng, D., Roberts, H.H., and Peckmann, J., 2011. Changing redox conditions at cold seeps as revealed by authigenic carbonates from Alaminos Canyon, northern Gulf of Mexico. *Chemical Geology*, 285(1): 82–96.
- Birgel, D., Thiel, V., Hinrichs, K.-U., Elvert, M., Campbell, K.A., Reitner, J., Farmer, J.D., and Peckmann, J., 2006. Lipid biomarker patterns of methane-seep microbialites from the Mesozoic convergent margin of California. *Organic Geochemistry*, 37(10): 1289–1302.
- Blumenberg, M., Seifert, R., Reitner, J., Pape, T., and Michaelis, W., 2004. Membrane lipid patterns typify distinct anaerobic methanotrophic consortia. *Proceedings of the national academy of sciences of the United States of America*, 101(30): 11111–11116.
- Blumenberg, M., Walliser, E.-O., Taviani, M., Seifert, R., and Reitner, J., 2015. Authigenic carbonate formation and its impact on the biomarker inventory at hydrocarbon seeps—A case study from the Holocene Black Sea and the Plio-Pleistocene Northern Apennines (Italy). *Marine and petroleum geology*, 66(3): 532–541.
- Blumer, M., Guillard, R.R.L., and Chase, T., 1971. Hydrocarbons of marine plankton. *Marine Biology*, 8: 183–189.
- Boetius, A., Ravensschlag, K., Schubert, C.J., Rickert, D., Widdel, F., Gieseke, A., Amann, R., Jørgensen, B.B., Witte, U., and Pfannkuche, O., 2000. A marine microbial consortium apparently mediating anaerobic oxidation of methane. *Nature*, 407: 623–626.
- Boetius, A., and Wenzhöfer, F., 2013. Seafloor oxygen consumption fueled by methane from cold seeps. *Nature Geoscience*, 6: 725–734.
- Budai, J.M., Martin, A.M., Walter, L.M., and Ku, T.C.W., 2002. Fracture-fill calcite as a record of microbial methanogenesis and fluid migration: a case study from the Devonian Antrim Shale, Michigan Basin. *Geofluids*, 2(3): 163–183.
- Campbell, K.A., 2006. Hydrocarbon seep and hydrothermal vent palaeoenvironments and paleontology: Past developments and future research directions. *Palaeogeography, Palaeoclimatology, Palaeoecology*, 232(2-4): 362–407.
- Chevalier, N., Bouloubassi, I., Birgel, D., Taphanel, M.H., and Lopez-Garcia, P., 2013. Microbial methane turnover at Marmara Sea cold seeps: a combined 16S rRNA and lipid biomarker investigation. *Geobiology*, 11(1): 55–71.
- Chien, C.W., Huang, C.Y., Chen, Z., Lee, H.C., and Harris, R., 2012. Miocene shallow-marine cold seep carbonate in fold-and-thrust Western Foothills, SW Taiwan. *Journal of Asian Earth Sciences*, 56: 200–211.
- Chien, C.W., Huang, C.Y., Lee, H.C., and Yang, K.M., 2013. Patterns and sizes of authigenic carbonate formation in the Pliocene foreland in southwestern Taiwan: Implications of an ancient methane seep. *Terrestrial atmospheric and oceanic sciences*, 24(6): 971–984.
- Chiu, J.K., Tseng, W.H., and Liu, C.S., 2006. Distribution of gassy sediments and mud volcanoes offshore southwestern Taiwan. *Terrestrial atmospheric and oceanic sciences*, 17(4): 703–722.
- Chung, C. T., 1962. Geology of the Hunghuatzu anticline, Kaohsiung, Taiwan. *Petroleum Geology of Taiwan*, 1: 31–50.
- Cranwell, P.A., Eglinton, G., and Robinson, N., 1987. Lipids of aquatic organisms as potential contributors to lacustrine sediments—II. *Organic Geochemistry*, 11: 513–527.
- Eglinton, G., and Hamilton, R.J., 1963. The distribution of alkanes. In: Swain, T. (Eds.), *Chemical Plant Taxonomy*. Academic Press, pp. 187–217.
- Eglinton, G., Hamilton, R.J., Raphael, R.A., and Gonzalez, A.G., 1962. Hydrocarbon constituents of the wax coatings of plant leaves: a taxonomic survey. *Nature*, 193(2): 739–742.
- Elvert, M., Suess, E., Greinert, J., and Whiticar, M.J., 2000. Archaea mediating anaerobic methane oxidation in deep-sea sediments at cold seeps of the eastern Aleutian subduction zone. *Organic Geochemistry*, 31(11): 1175–1187.
- Elvert, M., Suess, E., and Whiticar, M.J., 1999. Anaerobic methane oxidation associated with marine gas hydrates: superlight C-isotopes from saturated and unsaturated C_{20} and C_{25} irregular isoprenoids. *Naturwissenschaften*, 86(6): 295–300.
- Feng, D., Birgel, D., Peckmann, J., Roberts, H.H., Joye, S.B., Sassen, R., Liu, X.L., Hinrichs, K.-U., and Chen, D., 2014. Time integrated variation of sources of fluids and seepage dynamics archived in authigenic carbonates from Gulf of Mexico Gas Hydrate Seafloor Observatory. *Chemical Geology*, 385: 129–139.
- Feng, D., Peng, Y., Bao, H., Peckmann, J., Roberts, H.H., and Chen, D., 2016. A carbonate-based proxy for sulfate-driven anaerobic oxidation of methane. *Geology*, 44(12): 999–1002.
- Feng, D., and Roberts, H.H., 2010. Initial results of comparing cold-seep carbonates from mussel- and tubeworm-associated environments at Atwater Valley lease block 340, northern Gulf of Mexico. *Deep-Sea Research part II*, 57(21-23): 2030–2039.
- Giger, W., Schaffner, C., and Wakeham, S.G., 1980. Aliphatic and olefinic hydrocarbons in recent sediments of Greifensee, Switzerland. *Geochimica et Cosmochimica Acta*, 44(1): 119–129.
- Guan, H., Feng, D., Wu, N., and Chen, D., 2016b. Methane seepage intensities traced by biomarker patterns in authigenic carbonates from the South China Sea. *Organic Geochemistry*, 91: 109–119.
- Guan, H., Sun, Y., Mao, S., Zhu, X., and Wu, N., 2014.

- Molecular and stable carbon isotopic compositions of hopanoids in seep carbonates from the South China Sea continental slope. *Journal of Asian Earth Sciences*, 92: 254–261.
- Guan, H., Sun, Y., Zhu, X., Mao, S., Feng, D., Wu, N., and Chen, D., 2013. Factors controlling the types of microbial consortia in cold-seep environments: A molecular and isotopic investigation of authigenic carbonates from the South China Sea. *Chemical Geology*, 354: 55–64.
- Guan, H., Zhang, M., Mao, S., Wu, N., Lu, H., and Chen, D., 2016a. Methane seepage in the Shenhu area of the northern South China Sea: constraints from carbonate chimneys. *Geo-Marine Letters*, 36(3): 175–186.
- Harris, N.B., Freeman, K.H., Pancost, R.D., White, T.S., and Mitchel, G.D., 2004. The character and origin of lacustrine source rocks in the Lower Cretaceous synrift section, Congo Basin, West Africa. *AAPG Bulletin*, 88(8): 1163–1184.
- Himmler, T., Birgel, D., Bayon, G., Pape, T., Ge, L., Bohrmann, G., and Peckmann, J., 2015. Formation of seep carbonates along the Makran convergent margin, northern Arabian Sea and a molecular and isotopic approach to constrain the carbon isotopic composition of parent methane. *Chemical Geology*, 415: 102–117.
- Hinrichs, K.-U., Summons, R.E., Orphan, V., Sylva, S.P., and Hayes, J.M., 2000. Molecular and isotopic analysis of anaerobic methane-oxidizing communities in marine sediments. *Organic Geochemistry*, 31(12): 1685–1701.
- Huang, C.Y., Chien, C.W., Zhao, M., Li, H.C., and Iizuka, Y., 2006. Geological Study of active cold seeps in the syn-collision accretionary prism Kaoping slope off SW Taiwan. *Terrestrial atmospheric and oceanic sciences*, 17(4): 679–702.
- Huang, C.Y., Xia, K.Y., Yuan, P.B., and Chen, P.G., 2001. Structural evolution from Paleogene extension to Latest Miocene-Recent arc-continent collision offshore Taiwan: comparison with on land geology. *Journal of Asian Earth Sciences*, 19(5): 619–639.
- Judd, A., and Hovland, M., 2007. *Seabed Fluid Flow*, 475. Cambridge University Press, Cambridge.
- Lapham, L.L., Chanton, J.P., Martens, C.S., Sleeper, K., and Woolsey, J.R., 2008. Microbial activity in surficial sediments overlying acoustic wipeout zones at a Gulf of Mexico cold seep. *Geochemistry Geophysics Geosystems*, 9(6): 3043–3061.
- Li, J., Zhang, M., and Kong, T., 2017. New Discoveries of the Influence of Sedimentary Environment on Rearranged Hopanes in Source Rocks. *Acta Geologica Sinica* (English Edition), 91(2): 747–748.
- Lin, A.T., Watts, A.B., and Hesselbow, S.P., 2003. Cenozoic stratigraphy and subsidence history of the South China Sea margin in the Taiwan region. *Basin Research*, 15(4): 453–478.
- Meyers, P.A., 2003. Applications of organic geochemistry to paleolimnological reconstructions: a summary of examples from the Laurentian Great Lakes. *Organic Geochemistry*, 34 (2): 261–289.
- Mille, G., Asia, L., Guiliano, M., Malleret, L., and Doumenq, P., 2007. Hydrocarbons in coastal sediments from the Mediterranean Sea (Gulf of Fos area, France). *Marine pollution bulletin*, 54(5): 566–575.
- Naraoka, H., and Ishiwatari, R., 2000. Molecular and isotopic abundances of long-chain *n*-fatty acids in open marine sediments of the western North Pacific. *Chemical Geology*, 165(1): 23–36.
- Niemann, H., and Elvert, M., 2008. Diagnostic lipid biomarker and stable carbon isotope signatures of microbial communities mediating the anaerobic oxidation of methane with sulphate. *Organic Geochemistry*, 39(12): 1668–1677.
- Nöthen, K., and Kasten, S., 2011. Reconstructing changes in seep activity by means of pore water and solid phase Sr/Ca and Mg/Ca ratios in pockmark sediments of the Northern Congo Fan. *Marine Geology*, 287(1): 1–13.
- Peckmann, J., Birgel, D., and Kiel, S., 2009. Molecular fossils reveal fluid composition and flow intensity at a Cretaceous seep. *Geology*, 37: 847–850.
- Peckmann, J., and Thiel, V., 2004. Carbon cycling at ancient methane-seeps. *Chemical Geology*, 205(3): 443–467.
- Peters, K.E., and Moldowan, J.M., 1991. Effects of source, thermal maturity, and biodegradation on the distribution and isomerization of homohopanes in petroleum. *Organic Geochemistry*, 17(1): 47–61.
- Peters, K.E., Walters, C.C., and Moldowan, J.M., 2005. *The Biomarker Guide*. 2nd ed. Cambridge: Cambridge University Press. 1–1155
- Reeburgh, W. S., 1996. “Soft spots” in the global methane budget. In: Lidstrom, M.E., Tabita, F.R., (Eds.), *Microbial growth on C1 compounds*. Kluwer Academic Publishers, Dordrecht, the Netherlands, pp. 334–342.
- Reeburgh, W.S., 1976. Methane consumption in Cariaco Trench waters and sediments. *Earth and Planetary Science Letters*, 28: 337–344.
- Rohmer, M., Bouvier-Nave, P., and Ourisson, G., 1984. Distribution of hopanoid triterpenes in prokaryotes. *Journal of general microbiology*, 130(5): 1137–1150.
- Sackett, W.M., 1978. Carbon and hydrogen isotope effects during the thermocatalytic production of hydrocarbons in laboratory simulation experiments. *Geochimica et Cosmochimica Acta*, 42(6): 571–580.
- Simoneit, B.R.T., 1977. The Black Sea, a sink for terrigenous lipids. *Deep-Sea Research part II*, 24(9): 813–830.
- Suess, E., 2014. Marine cold seeps and their manifestations: Geological control, biogeochemical criteria and environmental conditions. *International journal of earth sciences*, 103(7): 1889–1916.
- Sung, Q., Lin, C.W., Lin, W.H., and Lin, W.C., 2000. Explanatory text of the geologic map of Taiwan scale 1:50,000; Sheet 51. Central Geological Survey, Ministry of Economic Affairs, Chiahhsien (Map).
- Suppe, J., 1984. Kinematics of arc-continent collision, flipping of subduction, and back-arc spreading near Taiwan. *Memoir of the Geological Society of China*, 6: 21–33.
- Taylor, J.D., and Glover, E.A., 2009. A giant lucinid bivalve from the Eocene of Jamaica - Systematics, life habits and chemosymbiosis (Mollusca: Bivalvia: Luciniidae). *Palaeontology*, 52: 95–109
- Thiel, V., Peckmann, J., Richnow, H.H., Luth, U., Reitner, J., and Michaelis, W., 2001. Molecular signals for anaerobic methane oxidation in Black Sea seep carbonates and a microbial mat. *Marine Chemistry*, 73(2): 97–112.
- Wang, Q.X., Tong, H.P., Huang, C-Y., and Chen, D.F., 2018. Tracing fluid sources and formation conditions of Miocene hydrocarbon-seep carbonates in the central Western Foothills, Central Taiwan. *Journal of Asian Earth Sciences*, 168:186–196.
- Wang, S.W., Gong, S.Y., Mii, H.S., and Dai, C.F., 2006. Cold-seep carbonate hardgrounds as the initial substrata of coral reef development in a siliciclastic palaeoenvironment of south-western Taiwan. *Terrestrial atmospheric and oceanic sciences*, 17(2): 405–427.
- Whiticar, M.J., 1999. Carbon and hydrogen isotope systematics of bacterial formation and oxidation of methane. *Chemical Geology*, 161(1-3): 291–314.
- Whiticar, M.J., Faber, E., and Schoell, M., 1986. Biogenic methane formation in marine and freshwater environments: CO₂ reduction vs. acetate fermentation - Isotope fermentation-Isotope evidence. *Geochimica et Cosmochimica Acta*, 50(5): 693–709.
- Zhang, M., Chen, J., and Jiang, L., 2017. Thermal Effects on Composition of Rearranged Hopanes in Hydrocarbon Source Rocks. *Acta Geologica Sinica* (English Edition), 91(1): 373–374.

About the first author



GUAN Hongxiang, female, born in 1981 in Hulun Beier City, The Inner Mongolia Autonomous Region; doctor; graduated from Graduate University of Chinese Academy of Sciences; associated professor of Guangzhou Institute of Energy Conversion, Chinese Academy of Sciences. She is now interested in using geochemistry as tools to study the geochemistry processes and methane cycling at cold seep systems. Email: guanhx@ms.giec.ac.cn; phone: 020-87076246.